


RESEARCH ARTICLE



A new tiny fossil penguin from the Late Oligocene of New Zealand and the morphofunctional transition of the penguin wing

Tatsuro Ando ^a, Jeffrey H. Robinson^b, Carolina Loch^c, Tamon Nakahara^d,
Shoji Hayashi^{d,e}, Marcus D. Richards^b and Robert Ewan Fordyce^{b†}

^aAshoro Museum of Paleontology, Ashoro, Japan; ^bDepartment of Geology, University of Otago, Dunedin, New Zealand; ^cSir John Walsh Research Institute, Faculty of Dentistry, University of Otago, Dunedin, New Zealand; ^dOkayama University of Science, Okayama, Japan; ^eDivision of Materials and Manufacturing Science, Graduate School of Engineering, Osaka University, Osaka, Japan

ABSTRACT

The Late Oligocene is a period of high penguin diversity, following major changes in the marine environment at the Eocene/Oligocene boundary and prior to the emergence of crown penguins in the Miocene. Historically, a large morphological gap existed between the most crownward *Platydyptes* among the Oligocene penguins from New Zealand and the Early Miocene stem penguins such as *Palaeospheniscus* from South America. Here we describe a new species that contributes to filling this gap. *Pakudyptes hakataramea* gen. et sp. nov. is the earliest tiny penguin, overlapping in size with the little penguin *Eudyptula minor*. Its distinctive combination of a well-developed proximal end of the humerus and an archaic elbow joint provides clues to the evolution of penguin wings. Phylogenetic analysis indicates that penguin wings evolved rapidly from the Late Oligocene to the Early Miocene, together with the acquisition of morphofunctional and hydrodynamical characteristics that enable the excellent swimming ability of modern penguins. As an indicator of aquatic adaptation, bone microanatomy shows a comparable structure to that of *Eudyptula*. The appearance of the smallest body size and the evolution of modern wings may have led to the ecological diversity of modern penguins, which confirms the importance of Zealandia in penguin evolution.

ARTICLE HISTORY

Received 21 July 2023
Accepted 24 May 2024

HANDLING EDITOR

Daniel Thomas

KEYWORDS

Smallest fossil penguin;
Latest Oligocene;
New Zealand; phylogeny;
evolution of wing

Introduction

Over the past two decades, studies of fossil penguins have revealed further details on their evolutionary history. These studies have not only described specimens which filled gaps in the fossil record, but also made significant advances in our understanding of their paleobiology (Ksepka et al. 2006; Slack et al. 2006; Clarke et al. 2010; Ksepka et al.

CONTACT Tatsuro Ando  ta@ashoromuseum.com; Jeffrey H. Robinson  jeff.robinson@otago.ac.nz

[†]Deceased

© 2024 The Author(s). Published by Informa UK Limited, trading as Taylor & Francis Group

This is an Open Access article distributed under the terms of the Creative Commons Attribution-NonCommercial-NoDerivatives License (<http://creativecommons.org/licenses/by-nc-nd/4.0/>), which permits non-commercial re-use, distribution, and reproduction in any medium, provided the original work is properly cited, and is not altered, transformed, or built upon in any way. The terms on which this article has been published allow the posting of the Accepted Manuscript in a repository by the author(s) or with their consent.

2012; Ando and Fordyce 2014; Acosta Hospitaleche and Reguero 2014; Mayr et al. 2017; Thomas et al. 2020; Jadwiszczak et al. 2021; Pelegrín and Acosta Hospitaleche 2022; Ksepka et al. 2023b). However, it is also true that there are still gaps to be filled, particularly with regard to the morphofunctional evolution of penguin wings.

Although the first penguin fossils were discovered in New Zealand (Mantell 1850) and the first described penguin was also from New Zealand (Huxley 1859), the fossil penguins from New Zealand that were studied in the early years were few (Hector 1871; Hector 1872; Oliver 1930) compared to fossil penguins from Eocene of Antarctica (Wiman 1905a; Wiman 1905b) and Miocene of South America (Ameghino 1891; Moreno and Mercerat 1891; Ameghino 1901; Ameghino 1905), which did not allow to elucidate the evolutionary history of penguins. Subsequent research has revealed the richness of New Zealand penguin fossils (Marples 1952; Simpson 1971; Fordyce and Jones 1990; Ando 2007; Ksepka et al. 2012; Ando and Fordyce 2014; Mayr et al. 2020; Thomas et al. 2023; Ksepka et al. 2023b). The penguin fauna from the Oligocene of Zealandia is especially rich, spanning a wide range of sizes and wing morphologies as well as showing high taxonomic diversity.

The phylogenetic relationships of New Zealand Oligocene penguins are congruently resolved in current phylogenetic analyses (Ksepka et al. 2012; Degrange et al. 2018; Thomas et al. 2020; Cole et al. 2022) with *Kairuku* being the most basal, followed by *Archaeosphenicus* and *Platydyptes*, which are followed by Early Miocene penguins from South America such as *Palaeospheniscus* and *Eretiscus*. The wings of *Palaeospheniscus* and *Eretiscus* have a similar structure to those of extant species (Moreno and Mercerat 1891; Simpson 1972; Acosta Hospitaleche et al. 2004; Acosta Hospitaleche et al. 2008) while *Platydyptes*, which is contemporary with *Pakudyptes*, has a wide humerus with a massive head, showing a large morphological gap between these penguins (Oliver 1930; Marples 1952; Ando 2007).

Here we describe a very small penguin from the Late Oligocene of New Zealand. It would have been similar in body size to the extant Little Blue penguin (*Eudyptula*, 40–45 cm length, 30–35 cm standing height; Simpson 1946; Reilly 1994), the Pliocene *Eudyptula wilsonae* (Thomas et al. 2023), and the Miocene *Eretiscus tonnii* (Simpson 1981). We herein refer to this smallest body size class as ‘tiny’ for penguins. The unique combination of a proximal end of the humerus that is as well developed as in extant species and a distal humerus and ulna that retain primitive features sheds new light on wing evolution in crown penguins.

The inclusion of the new penguin fossil in the phylogenetic analysis filled the morphological gap above. The analysis also revealed that changes in the penguin wing have occurred rapidly during this period. Kinematic and hydrodynamic studies (e.g. Bannasch 1994; Maeda et al. 2021; Harada et al. 2021; Hao et al. 2023; Shen and Tanaka 2023; Masud and Dabnichki 2023; Haidr 2023) could elucidate functional implications of this rapid change.

In addition to an analysis of its external features, we also conducted a study of the bone microstructure, which has been shown to play a crucial role in understanding how aquatic tetrapods have adapted to their aquatic environment (Houssaye et al. 2016). Penguins have highly dense osteosclerotic bones, which contribute to their buoyancy and diving abilities (Meister 1962; Ksepka et al. 2015). The term ‘aquatic adaptation’ we use here is based on an interpretation of bone microanatomy, meaning having dense

bones suitable for swimming and diving (e.g. Habib 2010; Houssaye et al. 2016). It should be noted that the relationship between microanatomical features and specific properties of aquatic adaptation in penguins is not yet clear, thus it is not possible to discuss whether ‘aquatic adaptation’ refers to diving depth, swimming style or foraging behaviour. Micro-anatomical changes associated with aquatic adaptation were not synchronised across the entire skeleton (e.g. Ksepka et al. 2015), indicating selective changes in bone density in specific regions.

The emergence of the smallest penguins from New Zealand during the morphofunctional transition of the penguin wing, and prior to the appearance of crown penguins may have significant implications for the evolutionary history of penguins.

Materials and methods

Three small penguin bones (OU 21976, OU 21977, and OU 21966) were collected in South Canterbury, New Zealand (Figure 1), by Craig M. Jones and R. Ewan Fordyce during a series of field trips in 1987 and deposited in the collections of the Geology Museum of the University of Otago. Institutional abbreviations for comparative specimens included in this study are: AMP, Ashoro Museum of Paleontology; CU, Canterbury University; MEF, Museo Paleontológico Egidio Feruglio; OM, Otago Museum; OU, The Geology Museum, Department of Geology, University of Otago; OUS, Okayama University of Science; USMN, The Smithsonian Institution, National Museum of Natural History. Measurements of the dimension were taken with a vernier caliper with 0.1 precision. Materials for comparison, table, and figures are listed in the supplementary information (<https://doi.org/10.5061/dryad.02v6wwq83>).

To investigate the phylogenetic position of the new fossil penguin described here as a new taxon, we added the taxon to the matrix of Ksepka et al. (2023b) with a few modifications (see supplementary information). The phylogenetic analysis for the

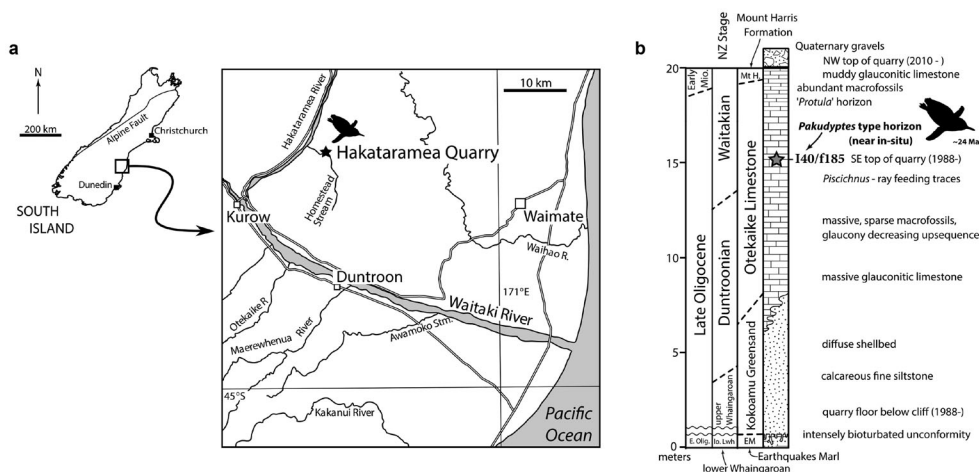


Figure 1. **a**, Simplified map of the South Island, New Zealand, showing the Waitaki Valley region and locality of *Pakudyptes* material (Hakataramea Quarry). **b**, Stratigraphy of Hakataramea Quarry with holotype horizon indicated. Images and data modified from Boessenecker and Fordyce (2017) following the stratigraphic revisions of Ksepka et al. (2023b).

revised matrix (71 taxa, 280 characters) was performed by TNT (Goloboff and Catalano 2016) using the 'New Technology Search' with default options except that 'find minimum length trees' was set to 10,000 times. This is the number obtained from preliminary trials, with reproducible results. Due to programme restrictions in TNT, the outgroup was set to *Gavia immer* only, and the 'ordered' characters in the original matrix are analysed as 'additive' characters. We mapped synapomorphies recovered in most parsimonious trees (MPTs hereafter) to selected nodes on a consensus tree to illustrate the morphological transition of penguins, especially the wing. Nodes where major changes occurred were labelled from A to F. Of these synapomorphies, those that are commonly recovered in all MPTs (unambiguous synapomorphies in PAUP/ common synapomorphies in TNT) can be used as a summary in character evolution studies (Goloboff et al. 2008).

Microanatomical data were acquired using two X-ray computed tomography (CT) scanners. The first scanner, located at the Faculty of Dentistry, University of Otago, New Zealand, was used to scan humeri and femora from extinct taxa, *Pakudyptes hakataramea* gen. et sp. nov. (OU 21977, OU 21966), *Platydyptes novaezealandiae* (OU 22003), and cf. *Palaeodyptes* (OU SI-REF 39, OU SI-REF 31) (Figure 4). The Orthophos Dentsply Sirona CBCT operated at 85 kV with a current of 5 and 7 mA (5 mA for *Platydyptes* and cf. *Palaeodyptes*, 7 mA for *Pakudyptes*). To accommodate the size limitations of the CT scanner, only the proximal/distal half of the humeri/femora were scanned for large specimens. The second scanner, a Latheta LCT-200 by Aloka, was located at Okayama University of Science in Okayama, Japan, and was used to scan humeri and femora from extant taxa, *Eudyptula minor* (OU AMP-R-56) and *Aptenodytes patagonicus* (OUS SH-K3) (Figure 4). This scanner operated at 80 kV with a current of 0.2 mA and had a resolution of 24 μm . To examine the bone microanatomy, longitudinal virtual sections were generated for each bone along the central axis of the medullary cavity. The acquired images were visualised, and virtual sections were performed using VGSTUDIO MAX, version 3.1 (Volume Graphics Inc).

A two-dimensional kinematic model for the movement of the caput humeri in the shoulder joint was reconstructed (Figure 6) to examine the range of pitch angle of rotation of the wing (feathering angle hereafter as in hydrodynamic terminology, e.g. Harada and Tanaka 2022) in stem penguins which have small torsional displacement (e.g. Simpson 1946). The model is based on the kinematic model for living penguins in Bannasch (1994), who demonstrated that the rotation of the caput humeri can be described as a two-axis eccentric motion. The first axis is the attachment of the ligamentum acrocoracohumerale to the coracoid, and the second axis is the attachment of the ligament to the caput humeri, the sulcus transversus as a pit in extant penguins (e.g. Figure 6a). The ligamentum acrocoracohumerale is always extended and acts like a lever (Bannasch 1994). The caput humeri rotates around the first axis while rotating around the second axis too, as well as sliding on the cavitas glenoidalis, and the feathering angle of the wing is the composite of these angles of rotation (Figure 6b–d). The rotation of the caput humeri can be determined by these axes, the trace of the movement on the caput humeri, and the position and axes of the scapular and coracoid lips of the cavitas glenoidalis. We reconstructed the model for stem penguins by changing the degree of the torsional displacement of the caput humeri.

The outline of the caput humeri drawn in Bannasch (1994) was positioned to have the same torsional displacement as that of the Eocene Antarctic stem penguin, OU SI-REF 39, with a line parallel to the cranial surface of the humerus as a representative of the wing angle (Figure 6e–g, h–j).

Systematic paleontology

AVES LINNAEUS, 1758

NEORNITHES GADOW, 1893 *SENSU* CRACRAFT, 1988

SPHENISCIFORMES SHARPE, 1891 *SENSU* CLARKE, ET AL., 2003

***Pakudyptes* gen. nov.**

Etymology. Māori, *paku*, small, and Greek, *dyptes*, diver as used in many names of penguins. Reference is to the small size and the character of wing-propelled diving.

Type species. *Pakudyptes hakataramea* sp. nov.

Included species. Type species only.

Locality. Hakataramea Quarry (44°39.50'S, 170°39.20'E, New Zealand Map Series NZMS 260 grid reference I40/237137), Hakataramea Valley, South Canterbury, New Zealand (Figure 1). That region has yielded abundant marine vertebrate fossils, including sharks, teleost fishes, cetaceans, and penguins (Simpson 1971a; Fordyce et al. 1982; Fordyce and Jones 1990; Gottfried et al. 2012; Tanaka and Fordyce 2014; Boessenecker and Fordyce 2017). Many of the Cenozoic fossil penguins in New Zealand were also found in this region (Simpson 1946; Marples 1952; Simpson 1971; Fordyce and Jones 1990). A *Platydyptes* cf. *marplei* specimen (OU 21997; field number REF 11-3-88-2; New Zealand Fossil Record File Database (www.fred.org.nz) number I40/f328) was collected from approximately the same horizon as the bones of *Pakudyptes* gen. nov.

Horizon. Otekaike Limestone, Waitakian, late Oligocene, ~ 24 Ma. The holotype of the type species and referred specimens were collected as float specimens on the top of the Otekaike Limestone of Hakataramea Quarry. It is important to note that the continued mining has now exposed an upward sequence since the time of collection. The horizon is the same as the micropaleontology sample I40/F185, which is in the *Globoquadrina dehiscentis* planktic foraminiferal biozone of Jenkins (1965) and the *Trachyleberis jillei* ostracod biozone of Ayress (Ayress 1993; Hornibrook 1996; Ksepka et al. 2023). The lower boundary of the Waitakian is ≥ 2 m below the horizon of the fossil (2020). The base of the Waitakian is constrained by strontium isotope dating to ~ 24.3 Ma, updated from Graham et al. (2000) using the LOWESS 6C strontium isotope curve calibration of McArthur et al. (2020).

Diagnosis. *Pakudyptes* is smaller than all other previously described penguin taxa except *Eudyptula* and *Eretiscus*. It differs from those penguins in having the following characters: bipartition of tricipital fossa is incomplete, shaft of humerus is narrow and straight with craniocaudally thick proximal portion, insertion scar for m. supracoracoideus is short and running parallel to the long axis of humerus, olecranon of ulna is round and tab-like.

***Pakudyptes hakataramea* sp. nov.**

Etymology. Māori, *hakataramea*, the enclosed valley basin, *ha-ka* (Kāi Tahu dialect), with speargrass (*Aciphylla squarrosa*), *ta-ra-me-a* (source: <https://kahurumanu.co.nz/>)

atlas accessed 22-11-2023). Reference is to the Hakataramea Valley where the holotype was collected.

Locality. As for the genus.

Horizon. As for the genus.

Holotype. OU 21977, nearly complete left humerus. Collected by R.E.F. on 16 October, 1987, when prospecting the rain-washed surface of the quarry.

Referred specimens. OU 21976, proximal half of the left ulna found within one metre from the holotype's collection site. They articulate well at the elbow joint, and are probably from the same individual. OU 21966, incomplete right femur, collected by Craig M. Jones on 23 May, 1987, at the same time as OU 21976. Both bones were within centimeters of each other loose on the quarry surface on the SE edge of the then-top platform of the limestone quarry. There is a high likelihood that all three specimens are the same individual and appear to all have been near in-situ. Even if the femur is not from the same individual, it is likely from the same species.

Remarks. The material described here was discovered in 1987 and reported as 'Hakataramea bird' in Fordyce and Jones (1990). Hakataramea bird was later suggested to be *Eretiscus*, a genus represented by another tiny penguin from the Early Miocene of South America (Cozzuol et al. 1991; Acosta Hospitaleche et al. 2004). Ando (2007) examined this penguin and determined it not to be *Eretiscus*.

Description

Humerus. The left humerus is almost complete, with a few small chips on the surface. The humerus length falls below the species average for *Eudyptula minor* and is 3.8 mm longer than the holotype of *Eretiscus tonnii* from the Early Miocene of Patagonia (Cozzuol et al. 1991; Acosta Hospitaleche et al. 2004) (Table 1). Despite being close in size to these species, the overall proportions are different. The proximal end is relatively small, and the shaft is narrow craniocaudally, resulting in a slender, elongated humerus compared to other tiny penguins (Figure 2).

The development of the proximal end is comparable to that of extant species. The ventral portion of the proximal end expands caudally resulting in the torsional displacement of the caput humeri and surrounding structures such as sulcus transversus, intumescentia humeri, and tuberculum ventrale. In proximal view, the articular surface is relatively smaller than that of *Eudyptula*. but the shape is comparable with the caudal margin, which is curved like a single arc. The caudal end of the articular surface tapers, making the curvature of the entire caput humeri stronger with the curved caudal margin.

Table 1. Dimensions (in mm) of humerus of *Pakudyptes hakataramea* gen. et sp. nov., *Eudyptula minor* (mean of 6 specimens), and *Eretiscus tonnii* (cast of MEF-PV 507). 1, Extreme length. 2, Diameter of head. 3, Width of shaft at 1/3. 4, Thickness of shaft at 1/3. 5, Width of shaft at 2/3. 6, Thickness of shaft at 2/3. 7, Width of distal end. 8, Thickness of distal end.

Species (specimen) (mm)	1	2	3	4	5	6	7	8
<i>Pakudyptes hakataramea</i> (OU 21977)	44.9	11.9	5.7	3.3	6.6	3.1	11.7	4.8
<i>Eudyptula minor</i> (n = 6)	46.0	12.4	6.9	3.2	8.2	2.9	14.6	4.7
<i>Eretiscus tonnii</i> (cast of MEF-PV 507)	42.2	10.2	5.4	3.1	7.3	2.7	11.8	4.0

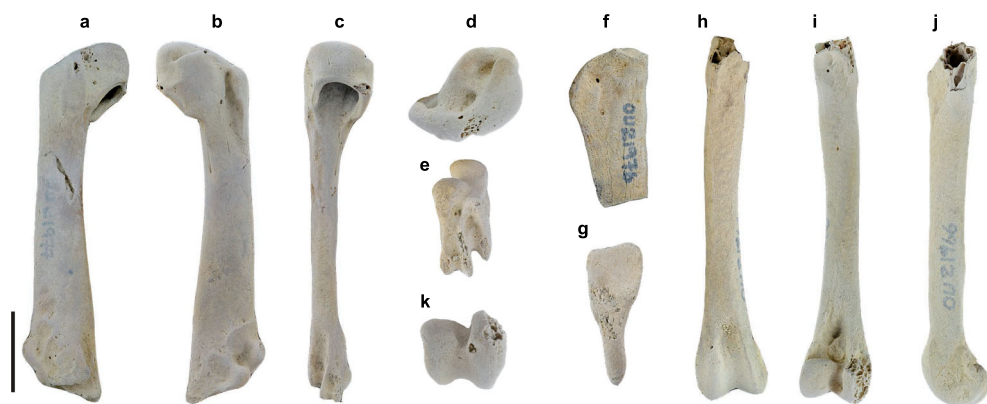


Figure 2. *Pakudyptes hakataramea* gen. et sp. nov. Left humerus (OU 21977) in **a**, cranial, **b**, caudal, **c**, ventral, **d**, proximal, and **e**, distal views. Left ulna (OU 21976) in **f**, caudal and **g**, proximal views. Right femur (OU 21966) in **h**, cranial, **i**, caudal, **j**, lateral, and **k**, distal views. Scale bar = 10 mm. **d**, **e**, **k**, and **g** are not to scale.

In caudal view, the shelf-like structure, on which the sulcus transversus lies as a distinct pit with an additional pit, is perpendicular to the long axis of the humeral shaft (Figure 2). The incisura capitis is shallow and less prominent that is not confluent with the sulcus. The tuberculum ventrale is slightly enlarged caudally, narrower than that in extant species.

The insertion scar for *m. supracoracoideus* is short reaching the level of the distal edge of the caudal portion of the fossa tricipitalis. The surface is elevated as seen in some stem penguins such as *Muriwaimanu tuatahi* (Slack et al. 2006). The scar is parallel to humeral shaft as in many stem penguins (Ando 2007; Ksepka et al. 2023). The insertion scar for *m. latissimus dorsi* is as proximal as that in extant penguins but because of the short insertion scar for *m. supracoracoideus*, the gap between these two scars is greater.

The fossa pectoralis forms a deeply excavated groove. The proximal end of the fossa is constricted by the expanded deltopectoral crest. The boundary of the tuberculum dorsale (insertion of *m. deltoideus minor*) at the proximal end of the crista deltopectoralis is less distinct. The tricipital fossa is wide and deep as in extant penguins, and is incompletely bipartite with a blunt rise, not a sharp ridge as seen in extant penguins. The rise does not extend to the cranial portion of the inside of the fossa.

The shaft is craniocaudally narrower proximally and wider distally, and is generally narrower than in *Eudyptula*, but the craniocaudal thickness is comparable to similar-sized *Eudyptula*. The caudal margin has a weak sigmoidal profile as in *Eudyptula*. The cranial margin has a slight bend which is weaker than that in *Eudyptula*. The bend barely reveals the proximal border of the insertion scar for *m. brachialis*.

The incisura intercondylaris is a deep notch between the caudal portions of these condyles as in extant penguins. The condylus dorsalis and condylus ventralis are positioned diagonally in distal view (Figure 2), as the condylus dorsalis is positioned dorsally, different from the condition in extant species in which they are aligned more craniocaudally (Figure 3). While the condylus dorsalis has a rather flat dorsal margin, the condylus ventralis is hemispherical with a distinct cranial margin. The caudodorsal margins are

rounded in both condyles. The incisura intercondylaris is a deep notch. The tangent of the condyles makes a smaller angle with the long axis of the humerus than that in extant species. As suggested by this angle, the reconstructed elbow joint is more flexed than in extant species when extended, condition as seen in stem penguins such as *Kairuku* (Ksepka et al. 2012).

The sulcus scapulotricipitalis and sulcus humerotricipitalis are deep grooves with high, plate-like crests forming the trochleae processes at the distoventral end of the humerus. The caudal process protrudes distoventrally as in other penguins, but the projection is shorter and blunter than that of extant species, not having a slight constriction.



Figure 3. Comparison of humeri, ulnae, and femora. **a–h**, *Eudyptula minor* (OU 22154). Left humerus in **a**, cranial, **b**, caudal, **c**, ventral, **d**, proximal, and **e**, distal views. Left ulna in **f**, caudal and **g**, proximal views. **h**, right femur (mirrored) in cranial view. **i–l**, *Eretiscus tonnii* (cast of MEF-PV 507). Left humerus in **i**, cranial, **j**, caudal, **k**, ventral, and **l**, distal views. **m–q**, *Platydyptes novaezealandiae* (OU 22003). Left humerus in **m**, proximal, **n**, caudal, and **o**, distal views. Left ulna in **p**, caudal and **q**, proximal views. **r–t**, cf. *Palaeudyptes* (OU SI-REF 39). Right humerus (mirrored) in **r**, proximal, **s**, caudal, and **t**, distal views. Scale bar = 10 mm. **d**, **e**, **g**, **l**, **m**, **o**, **q**, **r**, and **t** are not to scale.

In ventral view, the cranial bent is subtle, much weaker than in extant penguins. The caudal and middle ridges confluent proximally as in extant species. In cranial view, the cranial crest forms a triangular projection, and its proximal base recedes dorsally.

Ulna. The proximal half of the ulna is well-preserved except for subtle surface abrasions. The ulna is flattened craniocaudally, widest at the rounded, tab-like olecranon, and tapers distally in craniocaudal view. The olecranon is slightly deflected cranially in proximal view. The cotyla dorsalis is semicircular with a slightly convex caudal margin in the proximal view. The cotyla dorsalis is excavated hemispherically and bounded caudally with the crista intercotylaris. The edge of the crest is not as sharp as that in geologically older stem penguins such as *Kairuku*. The incisura radiale is very subtle. Humerus and ulna articulate well and are probably from the same individual.

Femur. The estimated length (~45 mm) is comparable to *Eudyptula* but the bone was more slender, consistent with the humerus. The shaft is straight craniocaudally and slightly curved mediolaterally. The cross section is circular in the middle and rather triangular in the proximal section as in extant penguins. The distal end is moderately expanded mediolaterally. The linea intermuscularis cranialis is continuous with the distolateral portion of the impressioes musculares trochanteris to the third fifth of the shaft where the line becomes untraceable. The linea intermuscularis caudalis is visible at the middle of the shaft, then bifurcates towards the crista supracondylaris lateralis and crista supracondylaris medialis.

The crista supracondylaris medialis is a moderate ridge as in *Eudyptula*, while the crista supracondylaris lateralis distinctly rises. The fossa poplitea is deep and distinct unlike extant penguins. The distal end is less expanded mediolaterally than other penguins. In distal view, the width of the distal end is almost equal to the height. The sulcus intercondylaris proximal to the impressio ligamentosus cruciati cranialis is shallow and there is almost no medial overhang of the lateral condyle. The impression is a distinct pit as in larger-sized extant penguins. The sulcus patellaris is moderately deep as in other penguins. In distal view, the crista lateralis is less pointed than the crista medialis and projects more anteriorly.

Microanatomy. The humeral sections of *Pakudyptes* demonstrate a thickening of the cortex (Figure 4) with a tubular diaphysis with a compact cortex surrounding a large, open medullary cavity; the cortex is thicker than in volant birds (Habib and Ruff 2008; Habib 2010; Ksepka et al. 2015). The thickness of the cortex gradually increases from the proximal to the mid-shaft and distal portions of the bone. The overall organisation in *Pakudyptes* appears similar to that of *Eudyptula* (Figure 4).

Platydyptes shows a tubular organisation with cortical thickening (Figure 4), sharing the tubular organisation with *Pakudyptes* though the degree of thickness is different. In '*Palaeudyptes*' and the extant King Penguin *Aptenodytes patagonicus*, a spongiosa fills the medullary space, resulting in the complete absence of a large, open medullary cavity (Figure 4).

In these humeri, the thickness of the cortex varies along the diaphysis, both proximal and distal to the mid-shaft, with a notable thickening around the growth centre (Figure 4). This pattern is observed in mammals, where the cortex is the thickest around the growth centre (Houssaye et al. 2018) and at the intersection of the nutrient arteries with the central axis of the medullary cavity (Houssaye and PrévotEAU 2020).

The internal organisation of the femur in *Pakudyptes*, *Platydyptes*, and '*Palaeudyptes*', exhibit a consistent pattern characterised by a large, open medullary cavity (Figure 4).



Figure 4. Longitudinal and midshaft cross-sections of humeri and femora. **a-d**, *Pakudyptes hakataramea* gen. et sp. nov. **a-b**, humerus (OU 21977). **c-d**, femur (OU 21966). **e-h**, *Eudyptula minor* (AMP-R-56). **e-f**, humerus. **g-h**, femur. **i-l**, *Platydyptes novaezealandiae* (OU 22003). **i-j**, proximal half of humerus. **k-l**, distal half of femur. **m-p**, cf. *Palaeudyptes*. **m-n**, proximal half of humerus (OU SI-REF 39). **o-p**, proximal half of femur (OU SI-REF 31). **q-t**, *Aptenodytes patagonicus* (OUS SH-K3). **q-r**, humerus. **s-t**, femur. Scale bars = 10 mm in **a, c, e, g, i, k, m, o, q, s** and 2 mm in **b, d, f, h, j, l, n, p, r, t**. OMC: open medullary cavity. In **i** and **o**, the medullary cavities are partially filled by matrix.

The relative thickness of the cortical bone in the femur was generally thinner than in humerus. The femur of *Pakudyptes* has a relatively thin cortical bone similar to that of *Eudyptula* (Figure 4). *Platydyptes* displays a thicker cortical bone and '*Palaeudyptes*'

has an even thicker cortical layer. The femur of *A. patagonicus* demonstrates an extremely compact and thick cortex, together with a compacted medullary region. In contrast to the fossil penguins studied, the femur of *A. patagonicus* lacks an open medullary cavity and instead has a relatively narrow zone with several irregularly shaped cavities that are separated by thick trabeculae (Figure 4).

Phylogenetic analysis

The phylogenetic analyses resulted in 92 MPTs with score 613, consistency index 0.626, and retention index 0.862. *Pakudyptes hakataramea* is recovered as a stem sphe-nisciform (Figure 5) one node crownward of *Platydyptes* spp. Following *Pakudyptes*, the next stem sphe-nisciform branch leads to the *Palaeospheniscus-Eretiscus* clade, *Marplesornis*, and then the crown Spheniciformes. The phylogenetic relationships of fossil penguins from the Oligocene to the Early Miocene were otherwise unchanged from previous studies.

Distribution of apomorphies

Morphological changes in the wing have been incremental, but significant changes occur at some nodes (Figure 5a). The largest change occurred at node A reflecting significant changes from volant birds to the flightless wing-propelled diving birds. However, such large changes have not necessarily occurred at the boundaries of geological epochs or across periods with poor fossil records.

Many key morphological transitions occur between Node C and Node D (Figure 5a). At node C, we observe unambiguous synapomorphies of crown penguins arise related to characters (162) shape of the head in dorsal view, (165) orientation of intumescencia humeri and tuberculum ventrale, (185) scar for origin of m. brachialis, (192) shelf adjacent to condylus ventralis, and (197) incisura radialis of ulna. At node D, three additional synapomorphies arise related to (169) the fossa tricipitalis, (173) distal extent of impressio insertii m. supracoracoideus and (180) foramen nutricum. After these changes, only one change is required up to the crown penguins and one more up to the extant species.

Results and discussion

Key morphofunctional transition of the wing in penguin evolution – Penguin wings have undergone major changes from the Oligocene to the present. *Pakudyptes*, with a combination of a modern proximal end and an archaic distal end of the humerus and proximal ulna, plays an important role elucidating such transitions.

A notable change observed in *Pakudyptes* is the development of the proximal end of the humerus, which is comparable to that of extant species. Its torsional displacement is large, and the caput humeri is caudally located. Such a modern-type proximal humerus occurs at node C (Figure 5). The degree of torsional displacement of the caput humeri may relate to the range of the pitch angle of rotation of the wing, or feathering angle (Figure 6a–c). Assuming the conditions other than the torsional displacement are constant, the range of the feathering angle shifted dorsally in the transition from stem

(Figure 6e–g) to crown penguins (Figure 6a–c). As another possibility, if the range of feathering angle has not changed, the position of the first axis and the angles of the scapular and coracoid lips of the cavitas glenoidalis would have changed significantly from stem (Figure 6h–j) to crown penguins (Figure 6a–c). A more conclusive evaluation requires the full reconstruction of the shoulder joint in stem penguins including the soft tissue; this is beyond the scope of this paper. Because the status in stem penguins

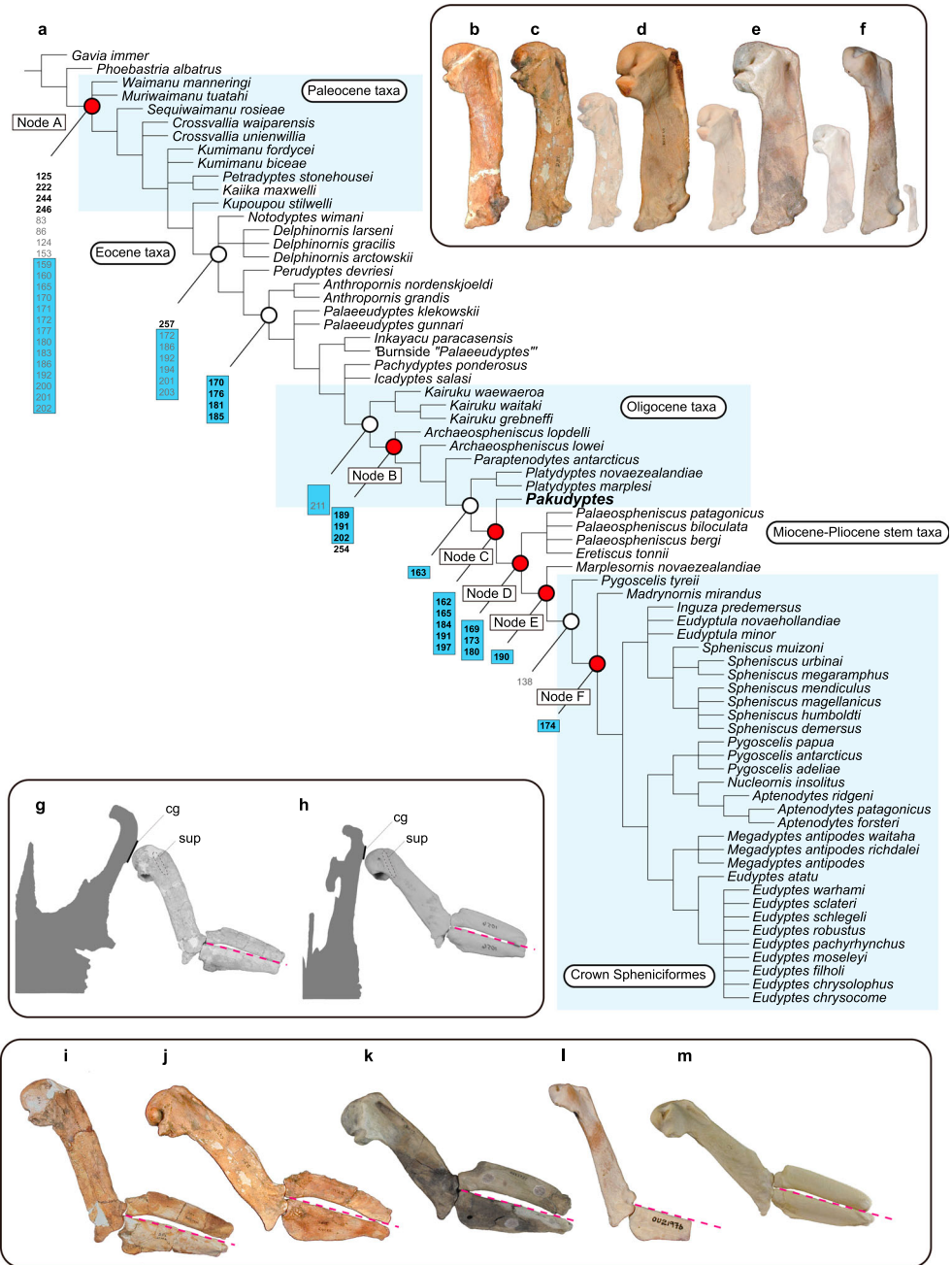


Figure 5. a, Strict consensus tree of the 92 MPTs resulting from the phylogenetic analysis, showing the relationships of *Pakudyptes hakataramea* gen. et sp. nov. with other Sphenisciformes. Synapomorphies are plotted on the selected node to illustrate the morphological transition of penguins, especially the wing. Empty circles are selected nodes, red circles are labelled nodes. Numbers in bold font are synapomorphies common to all MPTs (unambiguous synapomorphies in PAUP/ common synapomorphies in TNT), numbers in grey are synapomorphies not common to all MPTs. Blue filled areas are wing-related characters. **b–f**, Selected humeri in caudal view from the Oligocene New Zealand showing the morphological diversity. **b**, *Kairuku grebneffi* (OU 22065), right humerus, mirrored for comparison. **c**, *Archaeospheniscus lowei* (OM GL407), left humerus. **d**, *Platydyptes amiesi* (OU 22338), right humerus, mirrored for comparison. **e**, *Platydyptes marplei* (OU 22326), left humerus. **f**, *Pakudyptes hakataramea* (OU 21977), left humerus. Approximately scaled to have the same length. Semi-transparent images in **c–f** are sized relative to **b**, *Kairuku grebneffi* (OU 22065). **g–h**, Composite images of reconstructed shoulder joints of the left wing aligned to have the same forearm sweep angle in cranial view. Silhouettes of coracoid and sternum are made from images. **g**, *Kairuku* sp. (OM GL432, humerus) and *Kairuku grebneffi* (OU 22065, coracoid and sternum modified after Ksepka et al. 2012). **h**, *Aptenodytes forsteri* (CU 1054, mirrored humerus, and USNM 346257, coracoid and sternum), showing the articulated angles of sternum-coracoid, coracoid-humerus, and humerus-forearm elements (ulna and radius). Approximately scaled to have the same size. Dashed lines are support lines for the forearm elements (ulna and/or radius). sup, insertion scar for m. supracoracoideus. cg, area for cavitas glenoidalis. **i–m**, Reconstructed elbow joints of the left wing made of selected wing elements (humerus, ulna and/or radius) aligned to have the same forearm sweep angle in caudal view. **i**, *Kairuku* sp. (OM GL432). **j**, *Archaeospheniscus lowei* (OM GL407). **k**, *Platydyptes marplei* (OU 22935). **l**, *Pakudyptes hakataramea* (OU 21977, humerus, OU 21976, ulna). **m**, *Aptenodytes forsteri* (CU 1054). Approximately scaled to have the same size. Dashed lines are support lines for the forearm elements.

was unlikely to match either case exactly, it is highly probable that the actual status in stem penguins was somewhere between Figure 6e–g, h–j and the dorsal shift of the range of feathering angle also occurred to some extent at this part of the phylogeny. Since the feathering is the primary contributor to the thrust generation in the propulsion mechanism in penguins (Hao et al. 2023), the well-developed proximal humerus at node C may suggest that feathering motion at the shoulder joint was as optimised as in crown penguins. Other morphofunctional changes, as discussed below, occurred in different sections of penguin phylogeny.

In contrast to the more derived shoulder joint, the less derived elbow joint indicates that the wing of *Pakudyptes* is not morphologically and functionally equivalent to the modern penguins in many respects. The restriction of the caudal flexion (downward flexion in flapping motion) of the elbow joint makes the penguin wing a flipper that generates thrust by flapping motions. This restriction is primarily due to the flattening of the condyles at the distal end of the humerus. A flattening of the condyles similar to that of the extant species first occurs at node E. The rounded, spherical condyles of *Pakudyptes* and many stem penguins must have allowed a wider range of flexion. This would have been disadvantageous to thrust generation if compared to the wing of the extant species, since the greater the flexion, the less thrust produced by the upstroke.

The wing shape in its most extended state may be related to the propulsive function of the wing. Since the sweepback angle of a wing is closely related to its hydrodynamic property (see below). Extant species have relatively straight wings when extended (Simpson 1946), compared to many stem penguins such as *Muriwaimanu* (Mayr et al. 2020), *Kairuku* (Ksepka et al. 2012) and *Pakudyptes* (Figure 5). Such wings with a large

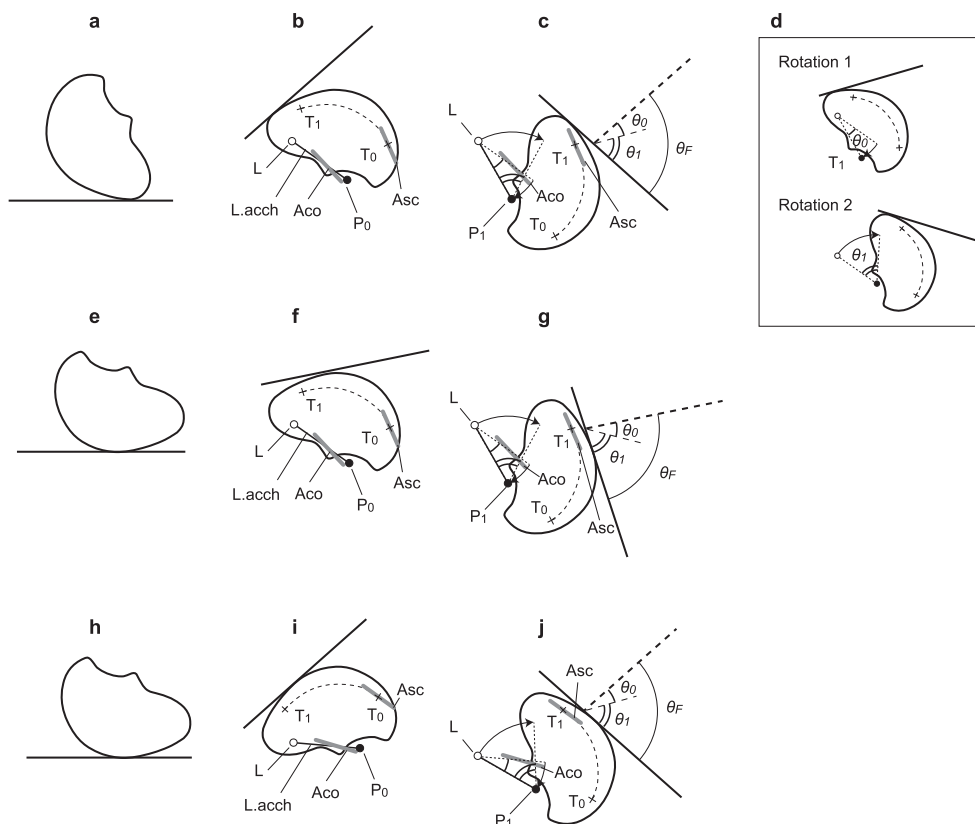


Figure 6. Two-dimensional kinematic models of the pitch angle of rotation, or feathering angle, of the penguin wing. **a–d**, model in crown penguins, redrawn after Bannasch (1994). **e–g**, model for stem penguins in which the outline was positioned to have the same torsional displacement as that of the Eocene Antarctic stem penguin, OU SI-REF 39 (Figure 3r). The positions of the first axis, which is the attachment of the ligamentum acrocoracohumerale to the coracoid, and the scapular and coracoid lips of the cavitas glenoidalis are same as in **a–d**. **h–j**, model for stem penguins in which the degree of the torsional displacement is same as in **e–g**, and the range of the feathering angle is same as in **a–d**. **a, e, h**, outline of the caput humeri as the proximal humerus is placed on a flat surface in proximal view. **b, f, i**, caput humeri at the end of the up-stroke of the wing. **c, g, j**, caput humeri at the end of the down-stroke of the wing. **d**, breakdown of the process from **b** to **c** depicting rotation 1 and rotation 2 separately. Note that rotation 1 and rotation 2 do not occur sequentially. The following abbreviations are based on Bannasch (1994) whenever possible. L, the first axis that is attachment of the ligamentum acrocoracohumerale to the coracoid; L. acch, ligamentum acrocoracohumerale that is always extended and act as a lever; P₀, the position of the second axis at the end of the up-stroke of the wing. The second axis is attachment of the ligament to the caput humeri (sulcus transversus as a pit); P₁, the position of the second axis at the end of the down-stroke of the wing; T₀, the starting point of the section of the trace of the movement of the caput humeri; T₁, the ending point of the section of the trace of the movement of the caput humeri; Aco, axis of the coracoid lip of the cavitas glenoidalis; Asc, axis of the scapular lip of the cavitas glenoidalis; Rotation 1, rotation around the first axis; Rotation 2, rotation around the second axis; θ_1 , angle of the rotation 1; θ_2 , angle of the rotation 2; θ_F , range of the feathering angle that is composite of θ_1 and θ_2 .

tangent angle of distal condyles occur at node B and are shared by all subsequent nodes except *Pakudyptes*. It becomes equivalent to the extant species at node D. The olecranon in the straighter wings is not tab-like. Instead, the ventral trochlear process is elongated, presumably to maintain an appropriate angle of force transmission from the extensors, m. humerotriceps and m. scapulotriceps. The diagonal insertion scar for m. supracoracoideus may also be related to the change in wing angle. The diagonal scar occurs at node D and is shared with crownward penguins. If the humerus has a larger angle to the body at the shoulder joint (Figure 5g–h), the angle of the scar should change to maintain a constant angle of force transmission from this powerful upstroking muscle. The forearm region influences the sweepback angle of the wing, which is a critical hydrodynamic property of the penguin wing including the achievement of optimal lift, the reduction of active buoyancy, and the efficient acquisition of thrust (Maeda et al. 2021; Hao et al. 2023). It is plausible that the change to straighter wings as seen in crown penguins is to maintain the optimal sweepback angle (Ksepka et al. 2012). This is consistent with the glenoid fossa of the coracoid facing more sternally in stem penguins (Ksepka et al. 2012).

It is puzzling that the phylogenetic position of *Pakudyptes* with an angled wing and straight scar for m. supracoracoideus breaks this pattern of wing evolution. The relatively straight wings may not have evolved in a straightforward manner. Future findings of fossil penguins and updated phylogenetic analyses would solve the issue. Here we note that the variation in wing angles may support this view. The holotype of *Platydyptes amiesi*, which is not included in the phylogenetic analysis performed here, seems to have a more angled wing than *P. novaezealandiae*, and there are differences in wing angles of extant penguins too, as Simpson (1946) commented. Our preliminary measurements (see supplementary information) show similar results, with *Aptenodytes* having the straightest wing and *Spheniscus* the most angled. This result suggests that the size and/or taxon correlates the angle. The variation among genera is greatest in *Eudyptula* with 10 degrees of difference.

The tricipital fossa is the origin of one of the extensor muscles for the forearm of the wing. The ventral head of m. humerotriceps originates from the interior of the tricipital fossa. The fossa of extant species is bipartite with a distinct ridge. Such a distinct ridge occurs at node D, although the relationship between the development of the ridge and the condition of the extensor muscles is uncertain.

The m. latissimus dorsi is one of the muscles associated with the wing upstroke (Banasch 1994). Its insertion becomes close to the scar for m. supracoracoideus at node F, as in extant species. The upstroke of the penguin wing not only provides acceleration performance independent of dive depth (Watanuki et al. 2006), enabling excellent swimming performance in deep dives (Kato et al. 2006), but also contributes to the penguin's turning maneuverability by generating centripetal forces (Harada and Tanaka 2022). The development of the upstroke function may have played an important role in the modernisation of the penguin wing. *Pakudyptes* has not acquired modern characteristics in this respect either.

Of the above wing transitions, the change from the Late Oligocene to the Early Miocene is particularly significant. Haidr (2023) demonstrated that wing variation in extant species reflects dietary preferences and the wing area is relevant to diving depth. Considering that the 'uniform' wings of extant species show such wide

ecomorphological variation, the functional and ecological diversity of penguins during these periods was much greater than expected.

Bone microanatomy – Microanatomical features such as cortical thickening and reduction of the medullary cavity are recognised as indicators of aquatic adaptation in tetrapods including penguins (Meister 1962; Chinsamy et al. 1998; Ksepka et al. 2015; Hous-saye et al. 2016). *Pakudyptes hakataramea* shares similar microanatomical features with *Eudyptula minor* (Figure 4). Their relatively thin cortices might be size-related, as smaller penguins have thinner bone walls when compared to larger penguins (Habib 2010). However, they are thicker than those of volant birds and (Habib and Ruff 2008), together with the condition of the humerus, show microanatomical features of penguins as diving birds. This suggests that *Pakudyptes*, whose body size is comparable to that of *Eudyptula*, had a comparable degree of aquatic adaptation in microanatomical context.

In *Pygoscelis adeliae*, sex-related differences in bone compactness have been documented, with females consistently demonstrating lower bone compactness than males (Garat et al. 2023). All individuals of *Eudyptula minor* observed for this study were male, yet they consistently displayed identical bone structure and compactness in both humeri and femora.

The contemporaneous, much larger *Platydyptes* (Marples 1952) has a thicker cortex and a smaller medullary cavity, suggesting a possible influence of body size on microanatomy. The humerus of the extant *Aptenodytes patagonicus* shows similar characteristics to the Eocene ‘cf. *Palaeudyptes*’, which exceeds the size of Emperor penguin *Aptenodytes forsteri*, suggesting a more specialised bone structure in extant penguins. This is supported by microanatomical features of the femora, where *A. patagonicus* has a significantly denser femur than fossil taxa, even exceeding the density of the much larger ‘cf. *Palaeudyptes*’. Variations in external morphology, such as the difference between the humerus of *Pakudyptes* and *Eudyptula*, do not necessarily correspond to microanatomical differences, as observed in other aquatic tetrapods (Hayashi et al. 2013).

In terms of the timing of the loss of a large open medullary cavity, the humerus shows a more derived adaptation to aquatic life than femur, suggesting that the densification of the wing bones preceded that of the femur in penguin evolution, as greater wing mass provides advantages for swimming or diving (Habib and Ruff 2008; Habib 2010). Conversely, Ksepka et al. (2015) analysed cross sections of the humerus, tibiotarsus, and femur in stem and crown penguins and showed that the hind limb reached the modern level of compactness before the humerus. However, recent studies have shown that longitudinal sections better represent the internal organisation of the bone (Hous-saye et al. 2018). For example, the femur of the Eocene ‘*Palaeudyptes*’ retains a large, open medullary cavity (Figure 4) despite the thick cortical layer. It should be noted that further comprehensive studies are needed to draw conclusions from these interpretations and to gain a deeper understanding of the sequence of adaptive changes in penguins.

Taxonomic and morphological diversity – Within Sphenisciformes, the taxonomic diversity of stem penguins was high in the Late Paleocene, Late Eocene, and Late Oligocene to Early Miocene, based on known fossil records (Ksepka and Ando 2011; Ando and Fordyce 2014; Thomas et al. 2020; Ksepka et al. 2023b). The

latter diversity follows drastic changes in the marine environment that occurred at the Eocene/Oligocene boundary and precedes the emergence of crown penguins resulting in the current high diversity (Ando and Fordyce 2014). Penguins from this period also show high morphological diversity, particularly in wing morphology, as discussed above. Most taxonomic and morphological diversity is observed in the medium to small penguins.

Pakudyptes hakataramea contributes to the high taxonomic and morphological diversity during this period. The combination of a modern proximal end and an archaic distal end makes *Pakudyptes* an unexpected penguin. This combination contrasts with *Archaeospheniscus* and *Platydyptes*, which have elbow joints closer to the crown penguins, and less developed shoulder joints than in *Pakudyptes*.

The extinction of giant penguins and the subsequent decline in taxonomic diversity may have been due to competition with emerging Neoceti, particularly odontocetes whose prey species compete with the larger penguins and which emerged in response to changes in the marine environment at the Eocene/Oligocene boundary (Ando and Fordyce 2014). This high selective pressure may also be responsible for the rapid evolution of wings and the appearance of the smallest penguin forms during this period.

The emergence of crown penguins was preceded by these changes. Factors such as mass extinctions and shifts in ecological strategies have been suggested to be associated with the reduction in body size (Jeschke and Kokko 2009; Montgomery and Mundy 2013; Wiest et al. 2015; Sallan and Galimberti 2015; Monarrez et al. 2021). The reduction in body size can lead to new body plans and the emergence of new taxa (Hanken and Wake 1993; Lee et al. 2014; Puttick et al. 2014), which may be the case with the emergence of crown penguins with modern-type wings. This scenario is consistent with the hypothesis that Zealandia was a key site for the emergence of crown penguins, not only for the early evolution of penguins (Thomas et al. 2020).

The tiniest extant penguin, *Eudyptula*, is much smaller than the smallest fully-aquatic endotherm (Downhower and Blumer 1988), probably due to the excellent thermal insulation provided by its feathers and the semi-aquatic life style (Stahel and Nicol 1982; Innes et al. 1989; Du et al. 2007). This would also be the case for the tiny-sized fossil penguins including *Pakudyptes* and *Eretiscus*. The lowest water temperature for *Eudyptula* species is 5 degrees Celsius (Stahel and Nicol 1982). It is true that all tiny penguin fossils are found in the temperate regions (Simpson 1971b, 1981; Acosta Hospitaleche et al. 2004; Ksepka and Thomas 2012; Thomas et al. 2023), but given climate fluctuations in the past (e.g. Zachos et al. 2001), this constraint may not necessarily apply to fossil penguins.

In crown penguins, morphological diversity is centred on beak morphology, which shows dietary diversification associated with the development of the Antarctic Circumpolar Current and the distribution of nutrient-rich prey, creating ecological diversity in current penguins (Olson 1985; Ando 2007; Thomas et al. 2020; Cole et al. 2022). The ability to exploit new ecological niches owing to smaller body size and the evolution of modern wings in the Late Oligocene-Early Miocene may have led to the ecological diversity of modern penguins.

Acknowledgments

We are grateful for the Foveran Station and Hakataramea Lime Quarry operators for permitting fieldwork and access. Thanks are extended to Diane Campbell, Charge medical radiation technologist, Radiology unit, Faculty of Dentistry University of Otago, for assistance with CBCT imaging of fossil penguins. Cody Phillips, On Lee Lau and Kane Fleury for facilitating access to modern penguin material at Tuhura Otago Museum. Craig Jones is thanked for his keen eye in spotting the two initial bone fragments on the quarry surface, and for sharing his fieldnotes with the authors. Many thanks to Gerald Mayr and an anonymous reviewer for their constructive and helpful comments.

Disclosure statement

No potential conflict of interest was reported by the author(s).

Funding

We gratefully acknowledge funding: a University of Otago Doctoral Scholarship to TA, and Grant 3542–87 and 3657–87 to REF from the National Geographic Society, Washington DC.

Data availability statement

The supplementary information is available from the Dryad Digital Repository <https://doi.org/10.5061/dryad.02v6wwq83>.

ORCID

Tatsuro Ando  <http://orcid.org/0000-0001-7553-5569>

References

- Acosta Hospitaleche C, Castro L, Tambussi CP, Scasso RA. 2008. *Palaeospheniscus patagonicus* (Aves, Sphenisciformes): new discoveries from the Early Miocene of Argentina. *J Paleontol.* 82(3):565–575. doi:10.1666/07-014.1.
- Acosta Hospitaleche C, Reguero M. 2014. *Palaeudyptes klekowskii*, the best-preserved penguin skeleton from the Eocene–Oligocene of Antarctica: taxonomic and evolutionary remarks. *Geobios.* 47(3):77–85. doi:10.1016/j.geobios.2014.03.003.
- Acosta Hospitaleche C, Tambussi CP, Cozzuol M. 2004. *Eretiscus tonnii* (Simpson) (Aves, Sphenisciformes): materiales adicionales, status taxonomico y distribucion geografica. *Revista del Museo Argentino de Ciencias Naturales.* 6(2):233–237. doi:10.22179/REVMACN.6.85.
- Ameghino F. 1891. Enumeración de las aves fósiles de la República Argentina. *Revista Argentina de Historia Natural.* 1(6a):441–453.
- Ameghino F. 1901. L'âge des formations sédimentaires de Patagonie. *Anales de la Sociedad Científica Argentina.* 51(6):20–91.
- Ameghino F. 1905. Enumeración de los Impennes Fósils de Patagonia y de la Isla Seymour. *Anales del Museo Nacional de Buenos Aires. Series.* 3:91–167.
- Ando T. 2007. New Zealand fossil penguins: origin, pattern, and process [dissertation]. Ewan Fordyce R, editor. University of Otago, Dunedin.
- Ando T, Fordyce RE. 2014. Evolutionary drivers for flightless, wing-propelled divers in the Northern and Southern Hemispheres. *Palaeogeography, Palaeoclimatology, Palaeoecology.* 400:50–61. doi:10.1016/j.palaeo.2013.08.002.

- Ayress MA. 1993. Ostracod biostratigraphy and palaeoecology of the Kokoamu Greensand and Otekaike Limestone (Late Oligocene to Early Miocene), North Otago and South Canterbury, New Zealand. *Alcheringa: An Australasian Journal of Palaeontology*. 17(2):125–151. doi:[10.1080/03115519308619491](https://doi.org/10.1080/03115519308619491).
- Bannasch R. 1994. Functional anatomy of the “flight” apparatus in penguins. In: Maddock L, Bone Q, Rayner JMV, editors. *Mechanics and physiology of animal swimming*. Cambridge: Cambridge University Press; p. 163–192.
- Boessenecker RW, Fordyce RE. 2017. Cosmopolitanism and Miocene survival of Eomysticetidae (Cetacea: Mysticeti) revealed by new fossils from New Zealand. *New Zealand Journal of Geology and Geophysics*. 60(2):145–157. doi:[10.1080/00288306.2017.1300176](https://doi.org/10.1080/00288306.2017.1300176).
- Chinsamy A, Martin LD, Dobson P. 1998. Bone microstructure of the diving *Hesperornis* and the volant *Ichthyornis* from the Niobrara Chalk of western Kansas. *Cretaceous Research*. 19(2):225–235. doi:[10.1006/cres.1997.0102](https://doi.org/10.1006/cres.1997.0102).
- Clarke JA, Ksepka DT, Salas-Gismondi R, Altamirano AJ, Shawkey MD, D’Alba L, Vinther J, DeVries TJ, Baby P. 2010. Fossil evidence for evolution of the shape and color of penguin feathers. *Science*. 330:954. doi:[10.1126/science.1193604](https://doi.org/10.1126/science.1193604).
- Cole TL, Zhou C, Fang M, Pan H, Ksepka DT, Fiddaman SR, Emerling CA, Thomas DB, Bi X, Fang Q, et al. 2022. Genomic insights into the secondary aquatic transition of penguins. *Nature Communications*. 13(1):3912. doi:[10.1038/s41467-022-31508-9](https://doi.org/10.1038/s41467-022-31508-9).
- Cozzuol MA, Fordyce RE, Jones CM. 1991. La presencia de *Eretiscus tonnii* (Aes, Spheniscidae) en el Mioceno temprano de Nueva Zelandia y Patagonia. *Ameghiniana*. 28:406.
- Degrange FJ, Ksepka DT, Tambussi CP. 2018. Redescription of the oldest crown clade penguin: cranial osteology, jaw myology, neuroanatomy, and phylogenetic affinities of *Madrynornis mirandus*. *Journal of Vertebrate Paleontology*. 38(2):e1445636. doi:[10.1080/02724634.2018.1445636](https://doi.org/10.1080/02724634.2018.1445636).
- Downhower JF, Blumer LS. 1988. Calculating just how small a whale can be. *Nature*. 335:675. doi:[10.1038/335675b0](https://doi.org/10.1038/335675b0).
- Du N, Fan J, Wu H, Chen S, Liu Y. 2007. An improved model of heat transfer through penguin feathers and down. *Journal of Theoretical Biology*. 248(4):727–735. doi:[10.1016/j.jtbi.2007.06.020](https://doi.org/10.1016/j.jtbi.2007.06.020).
- Fordyce RE. 1982. The fossil vertebrate record of New Zealand. In: Rich PV, Thompson EM, editors. *The fossil vertebrate record of Australasia*. Clayton: Monash Univ Offset Printing Unit; p. 629–698.
- Fordyce RE, Jones CM. 1990. Penguin history and new fossil material from New Zealand. In: Davis LS, Darby JT, editors. *Penguin biology*. San Diego: Academic Press; p. 419–446.
- Garat L M, Talevi M, Acosta Hospitaleche C. 2023. Osteohistology of the Antarctic penguin *Pygoscelis adeliae* (Aves, Sphenisciformes): definitive evidence of medullary bone. *Polar Biol*. 46(9):959–969.
- Goloboff PA, Catalano SA. 2016. TNT version 1.5, including a full implementation of phylogenetic morphometrics. *Cladistics*. 32(3):221–238. doi:[10.1111/cla.12160](https://doi.org/10.1111/cla.12160).
- Goloboff PA, Farris JS, Nixon KC. 2008. TNT, a free program for phylogenetic analysis. *Cladistics*. doi:[10.1111/j.1096-0031.2008.00217.x](https://doi.org/10.1111/j.1096-0031.2008.00217.x).
- Gottfried MD, Fordyce RE, Rust S. 2012. A new billfish (Perciformes, Xiphioidae) from the late Oligocene of New Zealand. *Journal of Vertebrate Paleontology*. 32(1):27–34. doi:[10.1080/02724634.2012.634471](https://doi.org/10.1080/02724634.2012.634471).
- Graham IANJ, Morgans HEG, Waghorn DB, Whitford DJ. 2000. Strontium isotope stratigraphy of the Oligocene-Miocene Otekaike Limestone (Trig Z section) in southern New Zealand: age of the Duntroonian / Waitakian Stage boundary. 43(3): 335–347. doi:[10.1080/00288306.2000.9514891](https://doi.org/10.1080/00288306.2000.9514891).
- Habib M. 2010. The structural mechanics and evolution of aquaflying birds. *Biological Journal of the Linnean Society*. 99(4):687–698. doi:[10.1111/j.1095-8312.2010.01372.x](https://doi.org/10.1111/j.1095-8312.2010.01372.x).
- Habib MB, Ruff CB. 2008. The effects of locomotion on the structural characteristics of avian limb bones. *Zoological Journal of the Linnean Society*. 153(3):601–624. doi:[10.1111/j.1096-3642.2008.00402.x](https://doi.org/10.1111/j.1096-3642.2008.00402.x).

- Haidr NS. 2023. Ecomorphological variation of the penguin wing. *Journal of Morphology*. 284(6): e21588. doi:10.1002/jmor.21588.
- Hanken J, Wake DB. 1993. Miniaturization of body size: organismal consequences and evolutionary significance. *Annual Review of Ecology and Systematics*. 24(1):501–519. doi:10.1146/annurev.es.24.110193.002441.
- Hao Z, Yin B, Prapamonthon P, Yang G. 2023. Hydrodynamic performance of a penguin wing: effect of feathering and flapping. *Phys Fluids*. 35:061907. <https://pubs.aip.org/aip/pof/article/35/6/061907/2897344>.
- Harada N, Oura T, Maeda M, Shen Y, Kikuchi DM, Tanaka H. 2021. Kinematics and hydrodynamics analyses of swimming penguins: wing bending improves propulsion performance. *Journal of Experimental Biology*. 224:jeb.242140. doi:10.1242/jeb.242140.
- Harada N, Tanaka H. 2022. Kinematic and hydrodynamic analyses of turning manoeuvres in penguins: body banking and wing upstroke generate centripetal force. *Journal of Experimental Biology*. 225(24):jeb.244124. doi:10.1242/jeb.244124.
- Hayashi S, Houssaye A, Nakajima Y, Chiba K, Ando T, Sawamura H, Inuzuka N, Kaneko N, Osaki T. 2013. Bone inner structure suggests increasing aquatic adaptations in desmostylia (mammalia, afrotheria). *PLoS One*. 8(4):e59146. doi:10.1371/journal.pone.0059146.
- Hector J. 1871. On the remains of a gigantic penguin *Palaeudyptes antarcticus* from the tertiary rocks on the west coast of Nelson. *Transactions and Proceedings of the New Zealand Institute*. 4:341–346.
- Hector J. 1872. Further notice of bones of a fossil penguin (*Palaeudyptes antarcticus*, Huxley). *Proceedings of the New Zealand Institute*. 4:438–439.
- Hornibrook NdB. 1996. New Zealand Eocene and Oligocene benthic foraminifera of the family notorotaliidae. *Institute of Geological and Nuclear Sciences Monograph*. 12:1–52.
- Houssaye A, Martin Sander P, Klein N. 2016. Adaptive patterns in aquatic amniote bone micro-anatomy—more complex than previously thought. *Integrative and Comparative Biology*. 56(6):1349–1369. doi:10.1093/icb/icw120.
- Houssaye A, PrévotEAU J. 2020. What about limb long bone nutrient canal(s)? - a 3D investigation in mammals. *Journal of Anatomy*. 236(3):510–521. doi:10.1111/joa.13121.
- Houssaye A, Taverne M, Cornette R. 2018. 3D quantitative comparative analysis of long bone diaphysis variations in microanatomy and cross-sectional geometry. *Journal of Anatomy*. 232(5):836–849. doi:10.1111/joa.12783.
- Huxley TH. 1859. On a fossil bird and a fossil cetacean from New Zealand. *Quarterly Journal of the Geological Society*. 15:670–677. doi:10.1144/GSL.JGS.1859.015.01-02.73.
- Innes S, Lavigne DM, Downhower JF, Blumer LS. 1989. Size of aquatic endotherms. *Nature*. 341:192. doi:10.1038/341192b0.
- Jadwiszczak P, Reguero M, Mörs T. 2021. A new small-sized penguin from the late Eocene of Seymour Island with additional material of *Mesetaornis polaris*. *GFF*. 143(2–3):283–291. doi:10.1080/11035897.2021.1900385.
- Jenkins DG. 1965. Planktonic foraminiferal zones and new taxa from the Danian to lower Miocene of New Zealand. *New Zealand Journal of Geology and Geophysics*. 8:1088–1126. doi:10.1080/00288306.1965.10428156.
- Jeschke JM, Kokko H. 2009. The roles of body size and phylogeny in fast and slow life histories. *Evol Ecol*. 23(6):867–878. doi:10.1007/s10682-008-9276-y.
- Kato A, Ropert-Coudert Y, Grémillet D, Cannell B. 2006. Locomotion and foraging strategy in foot-propelled and wing-propelled shallow-diving seabirds. *Marine Ecology Progress Series*. 308:293–301. doi:10.3354/meps308293.
- Ksepka DT, Ando T. 2011. Penguins past, present, and future: trends in the evolution of the sphenisciformes. In: Dyke G, Kaiser G, editors. *Living dinosaurs*. Hoboken: John Wiley & Sons Ltd; p. 155–186.
- Ksepka DT, Bertelli S, Giannini NP. 2006. The phylogeny of the living and fossil Sphenisciformes (penguins). *Cladistics*. 22:412–441. doi:10.1111/j.1096-0031.2006.00116.x.
- Ksepka DT, Field DJ, Heath TA, Pett W, Thomas DB, Giovanardi S, Tennynson AJD. 2023a. Largest-known fossil penguin provides insight into the early evolution of sphenisciform

- body size and flipper anatomy. *Journal of Paleontology*. 97(2):434–453. doi:[10.1017/jpa.2022.88](https://doi.org/10.1017/jpa.2022.88).
- Ksepka DT, Fordyce RE, Ando T, Jones CM. 2012. New fossil penguins (Aves, Sphenisciformes) from the Oligocene of New Zealand reveal the skeletal plan of stem penguins. *Journal of Vertebrate Paleontology*. 32(2):235–254. doi:[10.1080/02724634.2012.652051](https://doi.org/10.1080/02724634.2012.652051).
- Ksepka DT, Tennyson AJD, Richards MD, Fordyce RE. 2023b. Stem albatrosses wandered far: a new species of *Plotornis* (Aves, Pan-Diomedidae) from the earliest Miocene of New Zealand. *Journal of the Royal Society of New Zealand*. doi:[10.1080/03036758.2023.2266390](https://doi.org/10.1080/03036758.2023.2266390).
- Ksepka DT, Thomas DB. 2012. Multiple cenozoic invasions of Africa by penguins (Aves, Sphenisciformes). *Proceedings of the Royal Society B: Biological Sciences*. 279(1730):1027–1032. doi:[10.1098/rspb.2011.1592](https://doi.org/10.1098/rspb.2011.1592).
- Ksepka DT, Werning S, Sclafani M, Boles ZM. 2015. Bone histology in extant and fossil penguins (Aves: Sphenisciformes). *Journal of Anatomy*. 227(5):611–630. doi:[10.1111/joa.12367](https://doi.org/10.1111/joa.12367).
- Lee MSY, Cau A, Naish D, Dyke GJ. 2014. Sustained miniaturization and anatomical innovation in the dinosaurian ancestors of birds. *Science*. 345(6196):562–566. doi:[10.1126/science.1252243](https://doi.org/10.1126/science.1252243).
- Maeda M, Harada N, Tanaka H. 2021. Hydrodynamics of gliding penguin flipper suggests the adjustment of sweepback with swimming speeds. *bioRxiv*. 2021.05.24.445327. doi:[10.1101/2021.05.24.445327](https://doi.org/10.1101/2021.05.24.445327).
- Mantell G. 1850. Notice of the remains of the *Dinornis* and other birds, and of fossils and rock-specimens, recently collected by Mr. Walter Mantell in the Middle Island of New Zealand. *Quarterly Journal of the Geological Society*. 6:319–342. doi:[10.1144/GSL.JGS.1850.006.01-02.30](https://doi.org/10.1144/GSL.JGS.1850.006.01-02.30).
- Marples BJ. 1952. Early tertiary penguins of New Zealand. *New Zealand Geological Survey Paleontological Bulletin*. 20:1–66.
- Masud MH, Dabnichki P. 2023. Strouhal number analysis for the swimming of little penguin (*Eudyptula minor*): proof of efficient underwater propulsion. *Results in Engineering*. 17:100840. doi:[10.1016/j.rineng.2022.100840](https://doi.org/10.1016/j.rineng.2022.100840).
- Mayr G, Pietri D, Love VL, Mannering L, Bevitt AA, Scofield JJ, P R. 2020. First complete wing of a stem group sphenisciform from the paleocene of New Zealand sheds light on the evolution of the penguin flipper. *Diversity*. 12(2):46. doi:[10.3390/d12020046](https://doi.org/10.3390/d12020046).
- Mayr G, Scofield RP, De Pietri VL, Tennyson AJD. 2017. A Paleocene penguin from New Zealand substantiates multiple origins of gigantism in fossil Sphenisciformes. *Nature Communications*. 8(1):1–8. doi:[10.1038/s41467-017-01959-6](https://doi.org/10.1038/s41467-017-01959-6).
- McArthur JM, Howarth RJ, Shields GA, Zhou Y. 2020. Chapter 7 - Strontium isotope stratigraphy. In: Gradstein FM, Ogg JG, Schmitz MD, Ogg GM, editors. *Geologic time scale 2020*. Amsterdam: Elsevier; p. 211–238. doi:[10.1016/B978-0-12-824360-2.00007-3](https://doi.org/10.1016/B978-0-12-824360-2.00007-3).
- Meister W. 1962. Histological structure of the long bones of penguins. *The Anatomical Record*. 143:377–387. doi:[10.1002/ar.1091430408](https://doi.org/10.1002/ar.1091430408).
- Monarrez PM, Heim NA, Payne JL. 2021. Mass extinctions alter extinction and origination dynamics with respect to body size. *Proceedings of the Royal Society B: Biological Sciences*. 288(1960):20211681. doi:[10.1098/rspb.2021.1681](https://doi.org/10.1098/rspb.2021.1681).
- Montgomery SH, Mundy NI. 2013. Parallel episodes of phyletic dwarfism in callitrichid and cheirogaleid primates. *Journal of Evolutionary Biology*. 26(4):810–819. doi:[10.1111/jeb.12097](https://doi.org/10.1111/jeb.12097).
- Moreno FP, Mercerat A. 1891. Catálogo de los Pájaros fósiles de la República Argentina. *Anales del Museo de La Plata, Paleontología Argentina*. 1:8–71.
- Oliver WRB. 1930. *New Zealand birds*. Wellington: Fine Arts.
- Olson SL. 1985. The fossil record of birds. In: Farner DS, King JR, Parkes KC, editors. *Avian biology*. New York: Academic Press; p. 79–252.
- Pelegri n JS, Acosta Hospitaleche C. 2022. Evolutionary and biogeographical history of penguins (sphenisciformes): review of the dispersal patterns and adaptations in a geologic and paleoecological context. *Diversity*. 14(4):255. doi:[10.3390/d14040255](https://doi.org/10.3390/d14040255).
- Puttick MN, Thomas GH, Benton MJ. 2014. High rates of evolution preceded the origin of birds. *Evolution*. 68(5):1497–1510. doi:[10.1111/evo.12363](https://doi.org/10.1111/evo.12363).
- Reilly PN. 1994. *Penguins of the world*. South Melbourne: Oxford University Press.

- Sallan L, Galimberti AK. 2015. Body-size reduction in vertebrates following the end-Devonian mass extinction. *Science*. 350(6262):812–815. doi:[10.1126/science.aac7373](https://doi.org/10.1126/science.aac7373).
- Shen Y, Tanaka H. 2023. Experimental analysis of the sweepback angle effect on the thrust generation of a robotic penguin wing. *Bioinspiration & Biomimetics*. 18(2):026007.
- Simpson GG. 1946. Fossil penguins. *Bull Am Mus Nat Hist*. 87(1):7–99.
- Simpson GG. 1971a. A review of the pre-Pliocene penguins of New Zealand. *Bull Am Mus Nat Hist*. 144(5):319–378.
- Simpson GG. 1971. Fossil penguin from the late cenozoic of South Africa. *Science*. 171:1144–1145. doi:[10.1126/science.171.3976.1144](https://doi.org/10.1126/science.171.3976.1144).
- Simpson GG. 1972. Conspectus of Patagonian fossil penguins. *Am Mus Novit*. 2488:1–37.
- Simpson GG. 1981. Notes on some fossil penguins, including a new genus from Patagonia. *Ameghiniana*. 18(3–4):266–272.
- Slack KE, Jones CM, Ando T, Harrison GLA, Fordyce RE, Arnason U, Penny D. 2006. Early penguin fossils, plus mitochondrial genomes, calibrate avian evolution. *Molecular Biology and Evolution*. 23(6):1144–1155. doi:[10.1093/molbev/msj124](https://doi.org/10.1093/molbev/msj124).
- Stahel CD, Nicol SC. 1982. Temperature regulation in the little penguin, *Eudyptula minor*, in air and water. *J Comp Physiol*. 148:93–100. doi:[10.1007/BF00688892](https://doi.org/10.1007/BF00688892).
- Tanaka Y, Fordyce RE. 2014. Fossil dolphin *Otekaikea marplei* (Latest Oligocene, New Zealand) expands the morphological and taxonomic diversity of Oligocene cetaceans. *PLoS One*. 9(9): e107972. doi:[10.1371/journal.pone.0107972](https://doi.org/10.1371/journal.pone.0107972).
- Thomas DB, Ksepka DT, Holvast EJ, Tennyson AJD, Scofield P. 2020. Re-evaluating New Zealand's endemic Pliocene penguin genus. *New Zealand Journal of Geology and Geophysics*. 63(3):324–330. doi:[10.1080/00288306.2019.1699583](https://doi.org/10.1080/00288306.2019.1699583).
- Thomas DB, Tennyson AJD, Marx FG, Ksepka DT. 2023. Pliocene fossils support a New Zealand origin for the smallest extant penguins. *Journal of Paleontology*. 97(3):711–721. doi:[10.1017/jpa.2023.30](https://doi.org/10.1017/jpa.2023.30).
- Watanuki Y, Wanless S, Harris M, Lovvorn JR, Miyazaki M, Tanaka H, Sato K. 2006. Swim speeds and stroke patterns in wing-propelled divers: a comparison among alcids and a penguin. *Journal of Experimental Biology*. 209(Pt 7):1217–1230. doi:[10.1242/jeb.02128](https://doi.org/10.1242/jeb.02128).
- Wiest LA, Buynevich IV, Grandstaff DE, Terry DO, Maza ZA. 2015. Trace fossil evidence suggests widespread dwarfism in response to the end-Cretaceous mass extinction: Braggs, Alabama and Brazos River, Texas. *Palaeogeography, Palaeoclimatology, Palaeoecology*. 417:105–111. doi:[10.1016/j.palaeo.2014.10.034](https://doi.org/10.1016/j.palaeo.2014.10.034).
- Wiman C. 1905a. Über die alttertiären Vertebraten der Seymourinsel. *Wissenschaftliche Ergebnisse der Schwedischen Südpolar-Expedition*. 3(1):1–37.
- Wiman C. 1905b. Vorläufige Mitteilung über die alttertiären Vertebraten der Seymourinsel. *Bulletin of the Geological Institution of the University of Upsala*. 6(s):247–253.
- Zachos J, Pagani M, Sloan L, Thomas E, Billups K. 2001. Trends, rhythms, and aberrations in Global climate 65 Ma to present. *Science*. 292(5517):686–693.